Earthq Eng & Eng Vib (2021) 20: 969-979 **DOI**: https://doi.org/10.1007/s11803-021-2055-2

Theoretical analysis and experimental study on the dynamic behavior of a valve pipeline system during an earthquake

Xue Ruiyuan†, Yu Shurong†, ‡ and Zhang Xiheng§

College of Petrochemical Technology, Lanzhou University of Technology, Lanzhou 730050, China

Abstract: To study the dynamic behavior of pipeline systems installed with large-mass valves within nuclear power plants during earthquakes, seismic simulation tests are carried out on a pipeline system equipped with a DN80 gate valve, and the FEM updating technique is used to identify the stiffness distribution of the valve. By conducting tests and a numerical analysis, the following conclusions are obtained: After a large-mass valve is installed in the pipeline, the system shows higher sensitivity to intermediate and high frequency components in the earthquake than low frequency components. It is possible for the intermediate frequency components to be amplified by the valve in the horizontal direction, while the pipes tend to amplify the high frequency components in horizontal and vertical directions. Changes in the high-order modes of the system depend on valve stiffness distribution. Since the existence of a valve makes pipeline system damping distribute with an obvious non-proportional feature, when the response spectrum method is used to calculate the response of the pipeline system, it could result in an underestimation of low-damping positions and overestimation of high-damping positions.

Keywords: seismic analysis; shaking table test; valve; nuclear power plant

1 Introduction

Recently, when studying seismic risks where east-central nuclear power plants (NPPs) are located in the United States, researchers have found out that, compared with the response spectrum of the original safety shutdown at many other sites, the earthquake records at these sites contain higher frequency components (Mueller *et al*., 2015). Therefore, these researchers began to study the seismic capacity of nuclear power equipment under high frequency excitation (Gupta *et al*., 2019; Jeong *et al*., 2019). There are numerous valves and pipelines in NPPs that are classified into important grades for earthquake resistance. Scholars have conducted much research on the seismic performance of pipelines in NPPs. On one hand, it is hoped that the seismic margin of the pipelines could be improved, however, they are engaged in improving the damping value and the primary stress limitation of the seismic design of pipelines through the use of advanced analysis methods (Cho *et al*., 2019; Sinha *et al*., 2003; Surh *et al*., 2015; Zhang *et al*., 2015). In addition, the dynamic characteristic of the pipelines when considering fluid-solid coupling or solid-solid coupling has received extensive attention. For example, Paidoussis *et al*. (1974) studied the dynamics and stability of flexible pipes containing flowing flow and proposed the maximum allowable flow rate design criteria for pipes of different forms. Sinha *et al*. (2006) studied the seismic response of a core pipe in a submerged condition by combining an experiment and a finite element model (FEM) to update technology. Tang *et al*. (2018) studied the nonlinear fractional dynamics of pipes consisting of polymer materials under basic excitation. Deng and Yang (2019) discussed the propagation law of waves in immersed pipes that conveyed different fluids. Farajpour *et al*. (2019) first analyzed the buckling and post-buckling behavior of a fluid-conveying microtube in elastic media by using the modified couple stress theory. Manolisa *et al*. (2020) studied the seismic response of buried pipelines. Kheiri (2020) discussed the nonlinear dynamics of a fluid pipeline that had incomplete supports at the upstream end, but was free at the other end.

In the field of civil engineering, it is common to conduct seismic simulation experiments with the use of a shaking table to study the seismic performance of various structures (Xu *et al*., 2014; Xue *et al*., 2019). Nakamura (2013) reported the results of a shaking table test for a pipeline system containing various supports, but the frequency component of excitation in the test did not exceed 10 Hz, and the valves did not have an obvious effect on the dynamic characteristic of the system. The focus of the test centered on the pipeline. Kojima *et al*. (2017; 2018) studied the limit seismic capacity of an electric valve-driven mechanism based

Correspondence to: Yu Shurong, College of Petrochemical Technology, Lanzhou University of Technology, Lanzhou 730050, China
Tel: +86-931-2973728
E-mail: yusr@lut.edu.cn
†PhD; ‡Professor; §Associate Professor
Received November 25, 2019; **Accepted** August 12, 2020

on shaking table tests. Li *et al*. (2016) compared the effect of different types of excitation on test results resulting from a seismic identification test of valves. All the work mentioned above was focused on the limit seismic capacity of valves and pipelines or the dynamic characteristic of pipelines under special working conditions. The coupling between a valve and a pipeline was not considered in these studies, which would result in completely different seismic responses. In conclusion, limited by the performance of the shaking table and other conditions, the study on the dynamic behavior of the pipeline systems installed with large-mass valves, such as the main steam isolation valve pipeline system, during an earthquake is a largely unexplored field, especially when there are high frequency components in the excitation.

Generally, in engineering practice, the excitation is considered to be a high-frequency motion when main frequencies exceed 10 Hz (Nguyena *et al*., 2019). The author believes that for laboratory research, the effect of high frequency components can only be effectively studied if the high order modes of a system can be excited. In this paper, the system with a valve to pipes mass ratio of approximately 4 was established based on a DN80 gate valve. The dynamic behavior of the valve pipeline system during an earthquake was studied by combining numerical analysis and earthquake simulation tests. The high order modes of the system were excited by white noise and a sine sweep wave. Additionally, analyses were conducted on the hypothesis that deviation could be the cause in the process of the modeling of a valve pipeline system, as well as on the margin, caused by a calculation of seismic response by using the response spectrum method.

2 Model constructing

2.1 Design of the seismic simulation test

To study the coupling effect between a valve and a pipe in pipeline systems within NPPs, a pipeline system without an installing valve and a pipeline system with an installed valve were constructed, namely, structure I and structure II.

Structure I, as shown in Fig. 1, is a pipeline system that consists of two pipes that are connected by a pipe joint, with a total length of 3.5 m. The flange was welded to the end of the longer pipe, for convenience, in order to install the valve. Twelve accelerometers were absorbed in the system to measure structural responses. Both ends of the system and the supports were connected by nuts. The bottom plate of the support was fixed on the shaking table by eight M20 bolts. Welded by 30-mm thick steel plates, the supports have sufficient rigidity to transmit excitation of the shaking table to test structures. To guarantee that the resonance phenomenon could be observed during the experiment, the fundamental frequency of the test structures should be within the excitation frequency range of the shaking table. That is why the galvanized welded pipe with a specification of Φ48×3.5 mm was selected for this study. After the tests of structure I were completed, the valve was installed on the pipeline. Structure II was constructed as shown in Fig. 2. The valve was connected with the pipes by flanges, and the mass ratio between the valve and the pipes is about 4. Altogether, 16 measure points of the acceleration were distributed in structure II, among which A_8–A_{12} were distributed on the valve.

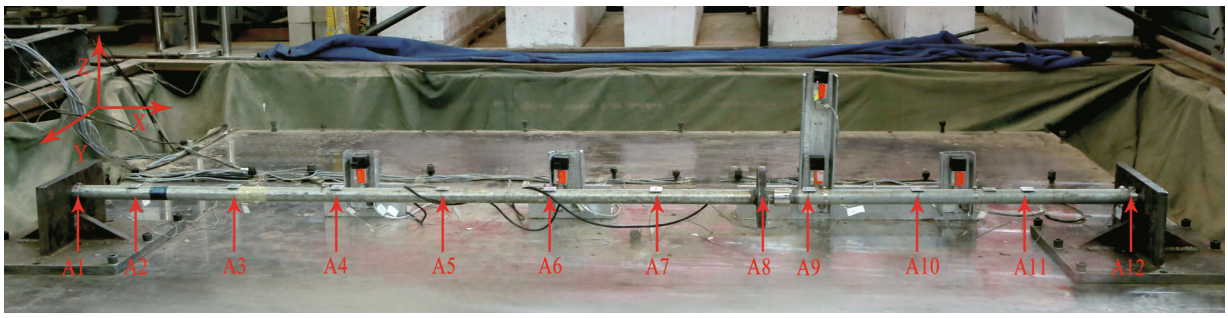

Fig. 1 The details of structure I and the arrangement of acceleration measuring points

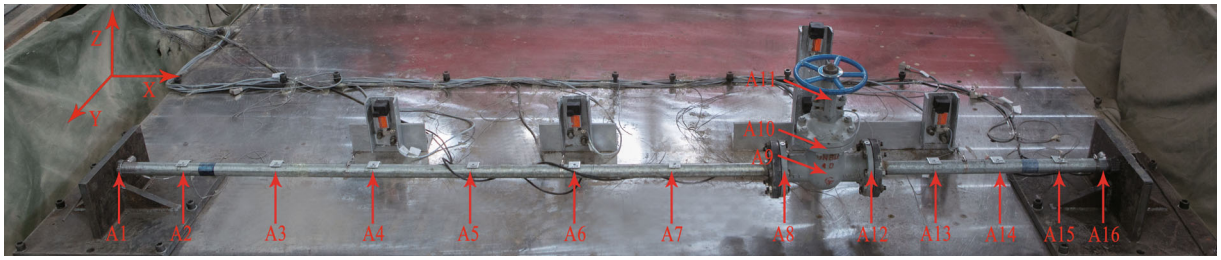

Fig. 2 The details of structure II and the arrangement of acceleration measuring points

This experiment used an electro hydraulic servo seismic simulated shaking table to provide excitation. The performance of the shaking table is shown in Table 1. The working conditions for the experiment are shown in Table 2. Since structure I is basically symmetrical, only direction *Y* was selected for tests, while due to the existence of a valve, the tests for structure II were conducted both in *Y* and *Z* directions. It should be noted that in the linear sweep tests, the frequency of the sine wave increases from 5 Hz to 50 Hz with a step size of 5 Hz, and the vibration duration of each frequency point was 10 s. The structures were located in the elastic region during the experiment.

2.2 Establishment of FEM

The lumped mass FEMs corresponding to the test structures are shown in Fig. 3. The positions of the nodes in the FEMs correspond to the positions of the accelerometers. The pipes were simulated by using massless pipe elements, and the supports were simulated by employing linear springs. If the valve is carefully modeled, the model will contain a large number of uncertainties. Therefore, massless beam elements were adopted to simulate the valve so as to replace all the uncertainties regarding parameters with clear physical meaning. The flexural rigidity of beam elements is used to equivalently simulate the rigidity distribution of the valve in direction *Y*, and compressive rigidity of the beam elements is used to equivalently simulate the rigidity distribution of the valve in direction *Z*. During the modeling process, the physical properties of the pipes and the spacing between the measure points are definite, and it could be that the translational constraints of the supports for the system are rigid constraints. However, according to relevant experiences (Sinha and Friswell, 2003; Sinha *et al*., 2006), the rotational constraints provided by the supports to the system were found to be not completely rigid. Therefore, for structure I, the uncertain parameters in the FEM include rotational rigidity of the linear spring, as well as flexural rigidity of element 8 corresponding to the pipe joint. For structure II, the uncertain parameters include rotational rigidity of the linear spring, plus flexural rigidity and compressive rigidity of the beam elements used to simulate the valve.

As the inverse algorithm of the FE method, the FEM updating theory is an effective method for identifying the uncertain parameters in FEM by using experimental data. Mottershead and Friswell (1993) introduced in

Table 1 Specifications of the shaking table

Table size	Frequency range	Maximum excitation amplitude	Degree of freedom
4 m × 4 m	0–50 Hz	20 m/s^2	Six degrees of freedom

Table 2 The details of test conditions

Number	Excitation waveform	Test structure	Excitation peak acceleration	Time-period
1	White noise	Structure I	1 m/s^2	120 s
2	*Y*-direction linearly sweep		3 m/s^2	100 s
3	*Y*-direction artificial seismic wave		10 m/s^2	60 s
4	White noise	Structure II	1 m/s^2	120 s
5	*Y*-direction linearly sweep		3 m/s^2	100 s
6	*Y*-direction artificial seismic wave		10 m/s^2	60 s
7	White noise		1 m/s^2	120 s
8	*Z*-direction linearly sweep		3 m/s^2	100 s
9	*Z*-direction artificial seismic wave		10 m/s^2	60 s

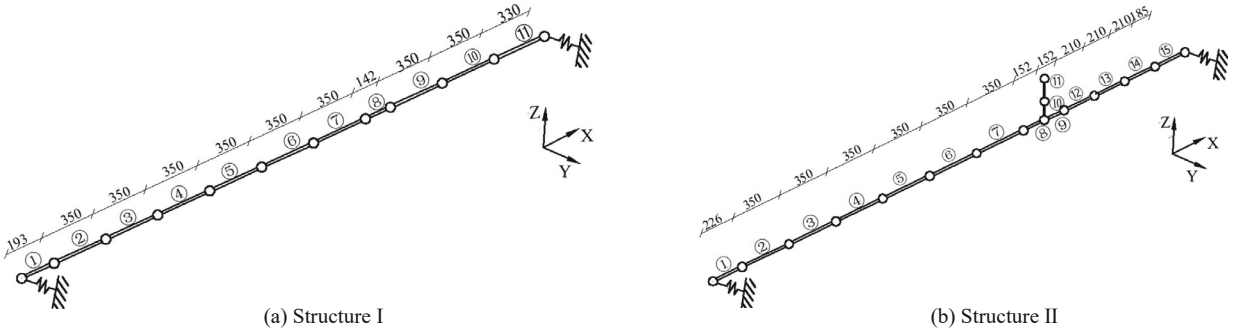

(a) Structure I (b) Structure II

Fig. 3 The lumped mass FEMs corresponding to the test structures (mm)

detail the development of the FEM updating method. Lin and Ewins (1994) proposed an FEM updating method based on frequency response function. Duan *et al*. (2004) proposed an improved FEM updating method to solve the condition in which the test modes were incomplete. Meanwhile, as a link between FEM and the actual structure, FEM updating technology has been widely used in the fields of online updating of uncertain parameters (Wang *et al*., 2018), damage diagnosis (Niu *et al*., 2015), health monitoring, and dynamic response prediction (Ashok and Shashi, 2015). Through the vibration control equation error-based FEM updating technique, the measured seismic responses in tests 3, 6 and 9 were used to identify the uncertain parameters in the FEMs corresponding to structure I, structure II in the *Y* direction, and structure II in the *Z* direction, respectively. The identification results are shown in Tables 3, 4 and 5, in which *E*, *I* and *A* represent, respectively, the modulus of elasticity, the inertia moment, and the cross-sectional area of the corresponding element.

As can be seen in Tables 3, 4 and 5, the supports could provide different rotational constraint intensity for structures I and II. This is because the outer extensions of the left and right ends of the pipes in different structures are different, and the connecting nuts between the supports and the pipes are processed and tightened manually. For structure II, constraints provided by the supports in the *Y* and *Z* directions are basically symmetrical, the connections between the valve and the pipes are not fully rigid, and the existence of the valve makes structure II show a quite different rigidity distribution in the *Y* and *Z* directions. The energy dissipation mechanism of the systems and the equipment within the NPPs is generally modeled by the use of Rayleigh damping. After the dynamic stiffness matrices of the test structures were accurately established, the Back Propagation neural network was used to identify the Rayleigh damping coefficients corresponding to structures I and II, with the maximum response value of each node under different damping distribution as the training set. The identification results are shown in Table 6 and Table 7, respectively.

The select upper and lower cutoff frequencies are 50 Hz and 5 Hz. If the damping ratio ε of the test systems is selected as 2%, then the corresponding theoretical α=1.097, β=1.14×10^{-4}. If ε is selected as 5%, then the corresponding theoretical α=2.74, β=2.85×10^{-4} (Naohiro, 2017). It can be seen from Table 6 and Table 7 that for structure I, compared to the theoretical damping coefficients of a 2% damping ratio, the damping coefficients of the pipes are smaller and the damping coefficients of the pipe joint element are larger. For structure II, the existence of the valve has made the damping distribution of the system show a significant non-proportional characteristic. The damping coefficients of the valve-related elements are higher than the theoretical one with a 5% damping ratio. The damping coefficients of the pipe-related elements are lower than the theoretical one with a 2% damping ratio, while the damping coefficients in the *Y* and *Z* directions are significantly different.

Table 3 Identification results of uncertain parameters for structure I

Uncertain parameters	Identification results
Rotating stiffness of left end spring K_{r1}	7.78×10^5 N·m/rad
Rotating stiffness of right end spring K_{r2}	1.397×10^5 N·m/rad
Flexural stiffness of element 8 E_8I_8	2.14×10^4 N·m^6

Table 4 Identification results of uncertain parameters for structure II (*Y* direction)

Uncertain parameters	Identification results
Rotating stiffness of left end spring K_{r1}	1.50×10^5 N·m/rad
Rotating stiffness of right end spring K_{r2}	1.49×10^5 N·m/rad
Flexural stiffness of elements 8 and 9 $E_8^YI_8^Y$	1.89×10^4 N·m^6
Flexural stiffness of element 10 $E_{10}I_{10}$	4.17×10^3 N·m^6
Flexural stiffness of element 11 $E_{11}I_{11}$	2.53×10^3 N·m^6

Table 5 Identification results of uncertain parameters for structure II (*Z* direction)

Uncertain parameters	Identification results
Rotating stiffness of left end spring K_{r1}	1.52×10^5 N·m/rad
Rotating stiffness of right end spring K_{r2}	1.48×10^5 N·m/rad
Flexural stiffness of elements 8 and 9 $E_8^ZI_8^Z$	4.03×10^4 N·m^6
Compressive stiffness of element 10 $E_{10}A_{10}$	1.75×10^6 N·m^4
Compressive stiffness of element 11 $E_{10}A_{10}$	1.77×10^5 N·m^4

Table 6 Identification results of damping coefficients for structure I

Element number	Mass damping coefficient α	Stiffness damping coefficient β
1, 2, 3, 4, 5, 6, 7, 9, 10, 11	1.018	8.08×10^{-5}
8	1.018	1.428×10^{-4}

Table 7 Identification results of damping coefficients for structure II

Element number	Mass damping coefficient α		Stiffness damping coefficient β	
	Y	*Z*	*Y*	*Z*
1, 2, 3, 4, 5, 6, 7	0.8	1	2.00×10^{-5}	6.00×10^{-5}
8, 9, 10, 11	3.5	3.5	4.02×10^{-4}	5.5×10^{-4}
12, 13, 14, 15	0.8	1	1.08×10^{-4}	6.05×10^{-5}

By comparing the power spectral density (PSD) curves of the theoretical responses calculated by the updated model with the PSD curves of the measured responses, we can verify whether the updated model can accurately predict the dynamic characteristics of the actual structure. To save space, only the theoretical and experimental PSD curves of measuring point 8 at the flange in structure I and measuring point 10 located in the middle of the valve in structure II are shown in Fig. 4.

As can be seen from Fig. 4, the theoretical PSD curves completely coincide with the measured PSD curves in shape, proving that the updated FEMs can accurately predict the dynamic characteristic of the actual structures. The slight difference between the two PSD curves on peak value is caused by the non-zero initial state of the test structures caused by the vibration of the driving oil pump of the shaking table.

In conclusion, in the modeling process of a pipeline system equipped with a larger-mass valve, the assumption to approximate the valve to a mass point and then to connect it rigidly to the pipe could cause a significant deviation between the model and the actual structure. The supports do not always provide full rigidity constraints to the system. In addition, different components in the pipeline system have different damping coefficients, and there are deviations between the theoretical and actual damping coefficients. Therefore, it is necessary to collect response data under the basic excitation of the nuclear pipeline systems during testing and operation at as many characteristic points as possible. This also applies to the basic excitation suffered by the system, so as to identify the uncertain parameters in the model by using FEM updating technology.

To successfully complete the identification process, the responses of the connection positions of the valve to the pipe and the responses of the center of gravity of the valve body, the valve drive mechanism, and the valve must be measured. For a pipeline, the arrangement density of measuring points can be adjusted according to the length of the pipeline. Meanwhile, a database that includes the updated model of common valves, connectors, supports and other components should be established, which could be used directly in modeling similar pipeline systems so as to improve the reliability of the analysis results.

3 Dynamic behavior analysis

3.1 Numerical analysis

It is difficult to measure the modes of structure I and structure II through experiment, but the modes can be obtained quickly by using updated FEMs. The theoretical modal information for the test structures is shown in Table 8.

It can be observed in Table 8 that after installing a large-mass valve in the pipeline, the each order natural frequency of the system will decrease significantly and the first order mode participation factors will be greatly increased. Note that the second order mode participation factor of structure II in the *Y* direction also increased slightly, while that of other higher order modes decreased to varying degrees. The position of each measuring point relative to the original state is used to represent the mass normalized mode shapes of structure I and structure II

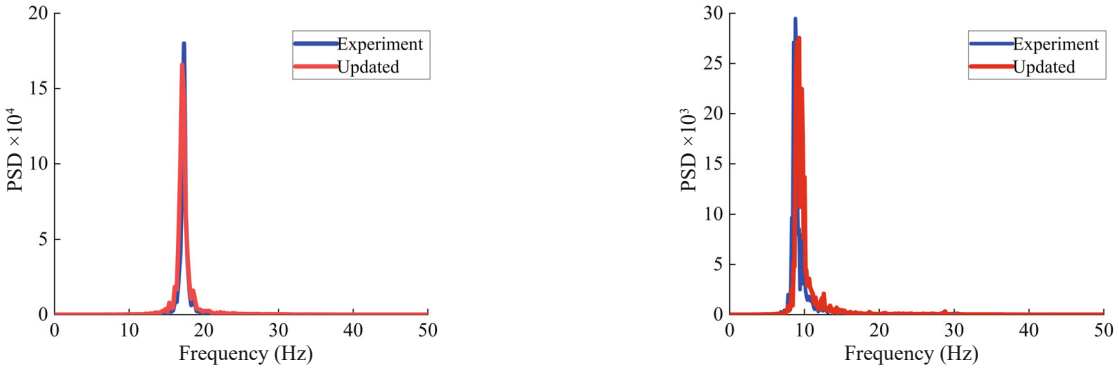

(a) Structure I (b) Structure II

Fig. 4 Comparison between theoretical and measured PSD curves

Table 8 The theoretical modal information of the test structures

	Structure I in the *Y* direction		Structure II in the *Y* direction		Structure II in the *Z* direction	
	Natural frequencies	Participation factors	Natural frequencies	Participation factors	Natural frequencies	Participation factors
First	17.2 Hz	3.88	9.0 Hz	7.40	8.9 Hz	7.41
Second	53.7 Hz	0.29	30.1 Hz	0.31	38.06 Hz	0.11
Third	122.7 Hz	1.47	43.9 Hz	0.61	69.9 Hz	0.043

that may be excited during the experiments. These are shown in Fig. 5.

As shown in Fig. 5, measuring points 7 and 5 in structure I are the positions with the maximum response when the first and second order modes of structure I are displayed. Despite the installation of the valve, both in the *Y* and *Z* directions, the pipes in structure II exhibit similar mode shapes to that of structure I, and the shape of the pipes is approximately symmetrical in the second and third order modes. Measuring points 7 and 5 are still the positions in the pipes with the highest response when the low order and high order modes are shown, as is the case in structure II. For the valve, the most obvious deformation occurs in the second order mode in the *Y* direction and the third order mode in the *Z* direction.

3.2 Experiment discussion

The dynamic behavior of the pipeline system during an earthquake was studied and discussed by calculating the PSD of the vibration measurement data in the experiment. The amplitude of the PSD curve is the measurement of time history, wave-carrying energy, which can directly represent the response strength of the test structures in different types of tests.

The PSD curves of the responses for the test structures in the direction *Y* are shown in Fig. 6, and the PSD curves in the direction *Z* appear in Fig. 7. Since the PSD values of the responses for structure I are far larger than those for structure II, for the convenience of observation the PSD values of structure I in Fig. 6(a) are multiplied by 0.05 and the PSD values of structure I in Figs. 6(b) and 6(c) are multiplied by 0.2. For brevity, combined with the research results in section 3.1, only the analysis results of measuring point 7 in structure I, the measuring points 5 and 7 in structure II as well as measuring point 11 on the top of the valve are presented.

From Fig. 6, it can be seen that during these three types of tests, structure I exhibits only the first order natural frequency, which is 17.5 Hz. From Fig. 6(a), it can be seen that three natural frequencies of 8.9 Hz, 30.5 Hz and 43.1 Hz can be observed in structure II during the white noise test, which can be considered corresponding to low, intermediate and high frequency components in the excitation. Under the excitation of white noise, which carries the same energy at each frequency point, measuring point 7 mainly amplifies low frequency components; measuring point 11 mainly amplifies the intermediate frequency components; and measuring point 5 mainly amplifies high frequency components. The PSD amplitude of measuring point 7 is far less than that of measuring points 5 and 11. Observation Fig. 6(b), in the *Y* direction linearly sweep test, structure II is mainly manifested as the first mode, and point 7 becomes the position with the largest response. Due to the short duration of the intermediate and high frequencies motions in the sweep wave, the high order modes of structure II were not obviously observed, but measurement points 11 and 5 still amplified the intermediate and high frequency components to some extent.

From Fig. 7(a), it is possible to observe that under the excitation of white noise, structure II exhibits two natural frequencies, of 8.9 Hz and 39.7 Hz in direction *Z*. It can be seen from Fig.7(b) that structure II also shows two order modes during the *Z*-direction linearly sweep test, indicating that the second order mode of the valve

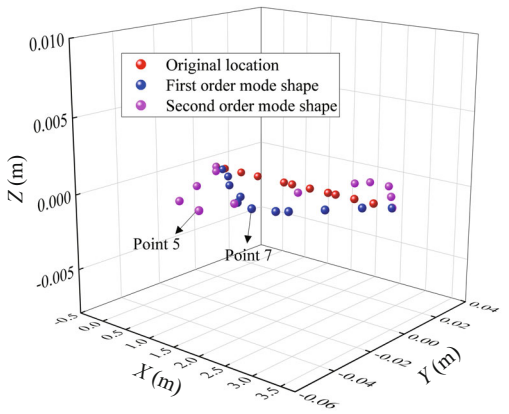

(a) The mode shapes of structure I in the *Y* direction

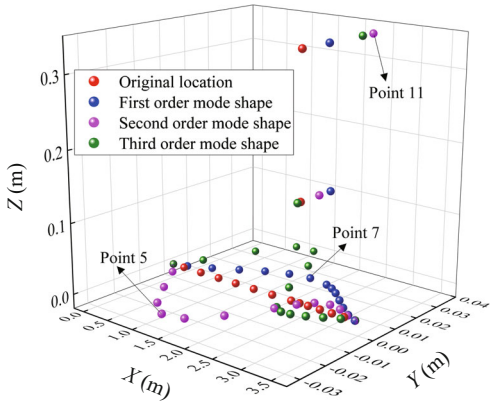

(b) The mode shapes of structure II in the *Y* direction

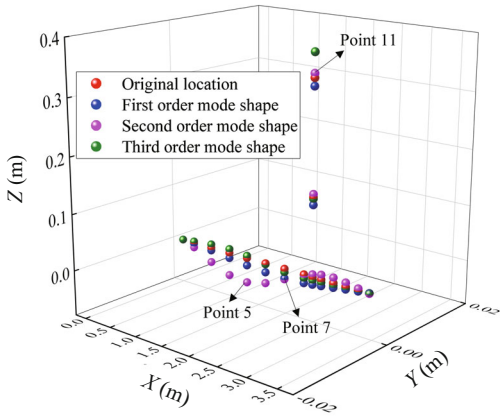

(c) The mode shapes of structure II in the *Z* direction

Fig. 5 Theoretical mode shapes of the test structures

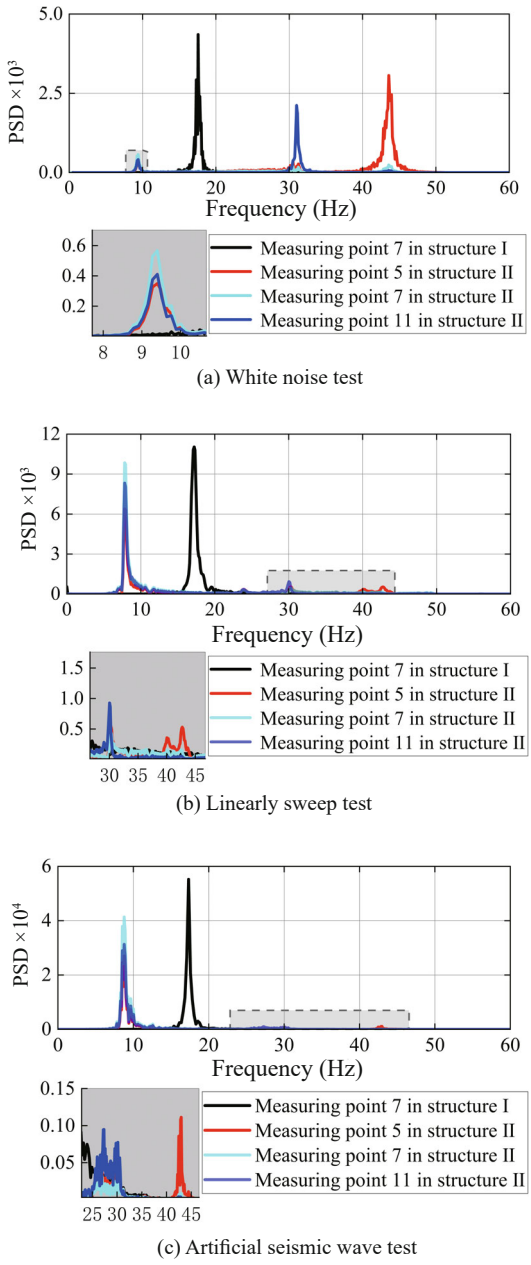

Fig. 6 Test measured PSD curves (*Y* direction)

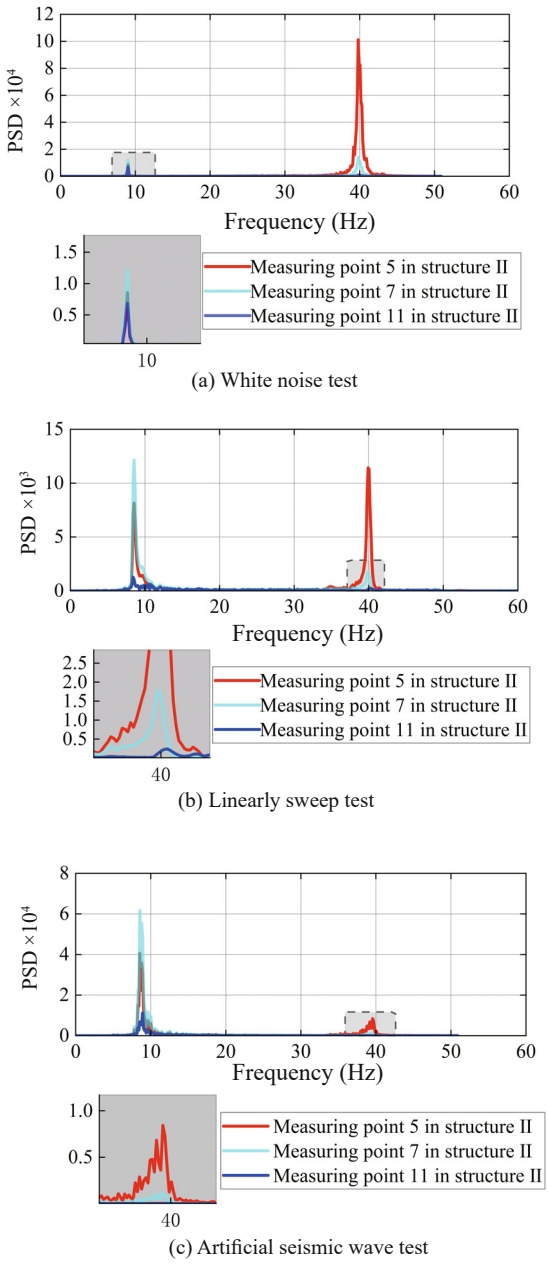

Fig. 7 Test measured PSD curves (*Z* direction)

pipeline system in the *Z* direction is easier to become excited. In the above two types of tests, measurement points 5 and 7 in structure II, respectively, amplify the high and low frequency components in the excitation, and the amplitudes of the PSD curve corresponding to measuring points 5 and 7 are greater than that observed in the *Y* direction. Due to large rigidity of the valve in the *Z* direction, this prevents the intermediate frequency components from being amplified. In addition, the responses of measuring point 11 are manifested only in low frequencies, and its PSD curve amplitude is less than in the Y direction.

In conclusion, the top of the valve has the largest response at intermediate frequencies and measuring point 7 closer to the valve has the largest response at low frequencies, while measuring point 5, situated farther from the valve, has the largest response at high frequencies. This indicates that the pipeline has different seismic vulnerabilities in different modes—that is, the input of seismic waves with different frequency components during seismic vulnerability analysis may lead to different results. The above experimental phenomena are consistent with the theoretical analysis results, which proves that it is feasible to infer the potential seismic vulnerabilities of the valve pipeline system directly from the theoretical mode shapes. The measured natural frequencies of the test structures are consistent with the theoretical natural frequencies listed in Table 8, which further proves the reliability of the updated FEMs.

The PSD curve of the artificial seismic wave used for the experiment is shown in Fig. 8.

As shown in Fig. 8, the artificial seismic wave is a broadband vibration with a vibration frequency band of 0–40 Hz. The frequency band with the maximum amount of energy is 10–15 Hz, and the energy level carried by frequencies above 30 Hz is relatively low. By observing Fig. 6(c) and Fig. 7(c), it can be observed that structure II mainly vibrates in the first order mode during artificial seismic wave tests. Measuring point 7 maximally amplifies the low frequency components of the excitation. The magnitude of magnification is 10^2. Meanwhile, measuring point 11 amplifies the intermediate frequency components of the excitation in direction *Y*, and measuring point 5 amplifies the high frequency components in directions *Y* and *Z*. The magnitudes of the magnification of both are also 10^2. These phenomena indicate that during the artificial seismic wave tests, the responses of structure II also contain high order modes. It can also be observed that under the excitation of an artificial seismic wave, the valve has a large response strength in direction *Y*, and the pipeline has a large response strength in direction *Z*. As the number of installed valves in the pipeline increases, it can be foreseen that the system will exhibit dynamic behavior during the artificial seismic wave tests, which is similar to behavior observed in the white noise tests or linearly sweep tests.

In brief, the dynamic behavior of the system formed after the installation of a large-mass valve in the pipeline becomes complicated during an earthquake. Although in the numerical analysis, the valve showed a greater response in the third mode in the *Z* direction, this mode is difficult to be excited by an actual earthquake in engineering practice. Therefore, it is concluded that the valve has a maximum response in the horizontal direction and can amplify the intermediate frequency components of the excitation only in the horizontal direction. The pipes have the largest response in the vertical direction and amplify the high frequency components of the excitation in both the horizontal and vertical directions. The system has a higher degree of amplification for the intermediate and high frequency components than for the low frequencies.

3.3 Influence pattern of a valve on dynamic characteristics of a pipeline system

The sensitivity of each uncertain parameter to the modes is calculated to analyze the influence pattern of the valve on the dynamic characteristic of the pipeline system. The sensitivity of physical parameters related to the structural dynamic characteristic with respect to various order modes can be calculated by Eq. (1):

$$\frac{\partial \lambda_j}{\partial \boldsymbol{\theta}} = \boldsymbol{\phi}_j^{\mathrm{T}} \left[\frac{\partial \boldsymbol{K}}{\partial \boldsymbol{\theta}} - \lambda_j \frac{\partial \boldsymbol{M}}{\partial \boldsymbol{\theta}} \right] \boldsymbol{\phi}_j \tag{1}$$

In Eq. (1), λ_j is the *j*-order natural frequency, ϕ_j is the *j*-order mass normalized vibration mode, $\boldsymbol{\theta}$ is the parameter vector, $\boldsymbol{K}$ and $\boldsymbol{M}$ are the stiffness matrix and the mass matrix. Sensitivities of all uncertain parameters in structure I and structure II to natural frequencies are shown in Tables 9, 10 and 11, in which $E_{\mathrm{p}}I_{\mathrm{p}}$ represents the flexural rigidity of pipe-related elements.

As can be seen from Tables 9, 10 and 11, whether or not the valve is installed in the pipeline, the parameter that has the greatest influence on the fundamental frequency of the pipeline system is the rigidity distribution of the pipeline. Certainly, if the constraint rigidity is small enough it could also generate significant influences on the dynamic characteristic. After a valve is installed in the pipeline, it is obvious that the stiffness distribution of the valve directly determines the change in the dynamic characteristic of the system. The value should be noted, given that, in most cases, the influence of the pipe stiffness distribution on the dynamic characteristic increases with an increase of valve stiffness. For structure II, the change of the fundamental frequency in direction *Y* is determined by the flexural rigidity of the parallel part of the valve and the pipes, that is, elements 8 and 9. In addition, the flexural rigidity of the bonnet, the hand wheel, the vertical part of the valve body and other parts, that is, elements 10 and 11, directly determine the changes of the second and third order modes. In direction *Z*, since the valve exhibits large compressive rigidity, its influence on the modes is reduced sharply, but the compressive rigidity of the hand wheel, packing gland and other components located at the top of the valve determine the changes of the third order mode.

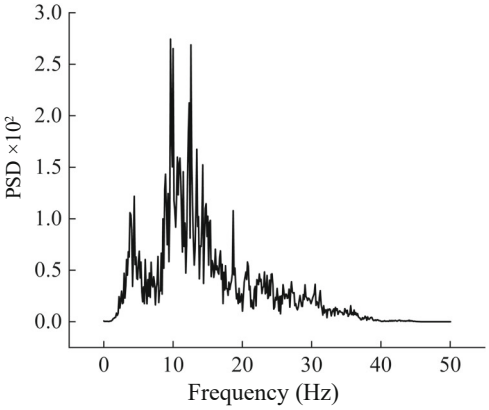

Fig. 8 PSD curve of the artificial seismic wave

Table 9 Sensitivity of uncertain parameters to the modes for structure I

The modal number	K_{r1}	K_{r2}	$E_8 I_8$	$E_{\mathrm{p}} I_{\mathrm{p}}$
First	0.00039	0.014	0.0364	0.304
Second	0.0062	0.0429	0.4792	3.24
Third	0.021	0.45	0.0557	17.91

4 Margin analysis of the response spectrum method

Seismic analysis of pipelines still adopts the response spectrum method to predict the structure response. The ratio of the calculated result by using the response spectrum method to the maximum value of the measured absolute acceleration is defined as the margin of the response spectrum method, expressed by κ. The response spectrums corresponding to the artificial seismic wave at different damping ratios are shown in Fig. 9. The margin of the results obtained by using the response spectrum method to predict the seismic responses of test structures under conditions 3, 6 and 9, shown in Table 2, are drawn in Fig. 10, in which the damping ratio of structures I and II adopts 2% and 5%, respectively. The points inside the rectangle in Fig. 10 are the valve related measuring points in structure II.

It can be seen from Fig. 10 that for structure I, since the actual damping ratio is less than 2%, the margin for each measuring point calculated by response spectrum method is less than 1.

For structure II, the predicted results of valve-related measuring points have large margins, but the margins of the predicted results for pipe-related measuring points are close to 1 or smaller than 1. This is because the damping distribution in structure II has an obvious non-proportional characteristic, that is, the actual damping ratio of the valve is larger than 5% and the actual damping ratio of the pipes is smaller than 2%. However, in a calculation using the response spectrum method, a 5% damping ratio is adopted, resulting in the overestimation of valve responses and the underestimation of pipes responses. In short, the characteristic of the damping distribution of the system and the damping level selected in the calculation determine the margin of the results calculated using the response spectrum method. In the calculation using the response spectrum method, the reliability of the predicted results could be enhanced by selecting response spectrums with different damping ratios for different parts of the structure.

5 Conclusion

To make up for the lack of research on the dynamic behavior of the pipeline system installed with large-mass valve in NPPs during an earthquake, the pipeline system with a valve to pipeline mass ratio of about 4 was established in this essay for the seismic simulation test and numerical analysis and the following conclusions were obtained:

1) In the process of establishing the FEM of the valve piping system, the responses of the system under basic

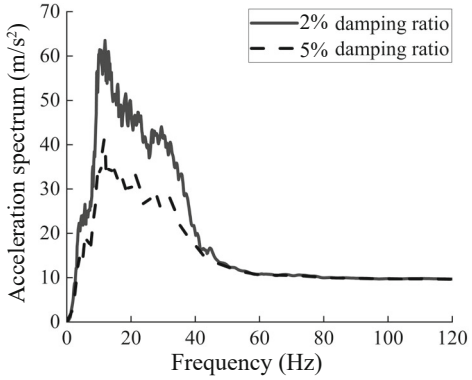

Fig. 9 Response spectrum of artificial seismic wave

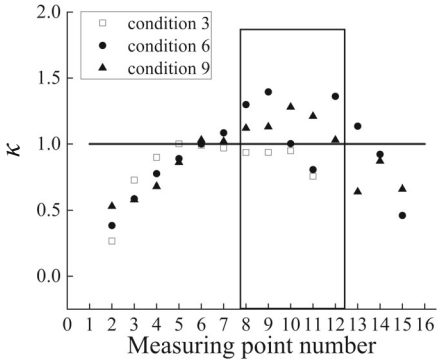

Fig. 10 Margin of response spectrum prediction results

Table 10 Sensitivity of uncertain parameters to the modes for structure II (*Y* direction)

The modal number	K_{r1}	K_{r2}	E_8I_8	$E_{10}I_{10}$	$E_{11}I_{11}$	E_pI_p
First	0.0021	0.0050	0.029	0.0060	0.0014	0.049
Second	0.032	0.0046	0.27	2.16	1.02	0.59
Third	0.081	0.0018	0.39	5.19	3.84	1.17

Table 11 Sensitivity of uncertain parameters to the modes for structure II (*Z* direction)

The modal number	K_{r1}	K_{r2}	E_8A_8	$E_{10}A_{10}$	$E_{11}A_{11}$	E_pI_p
First	0.0023	0.0030	0.0069	0.0000023	0.000028	0.077
Second	0.083	0.0095	0.177	0.00013	0.0027	1.55
Third	0.0062	0.0011	0.0083	0.0051	1.008	0.16

excitation should be collected and the FEM updating method should be used to identify the uncertainties, such as the valve stiffness distribution and the constraint strength. If the valve and the pipe are set as a rigid connection, it could distort the analysis results.

2) The second order mode of the valve pipeline system in the vertical direction was more easily excited than the one in the horizontal direction. Under the earthquake action with the same intensity, the pipeline had a larger response in the vertical direction and the valve had a larger response in the horizontal direction.

3) The system formed by installing a valve with large-mass in the pipeline showed a higher sensitivity to the intermediate and high frequency components of earthquake excitation than the low frequency components. It is possible for the intermediate frequency components of earthquake excitation to be amplified horizontally by the valve, while the high frequency components may be amplified by pipes in both horizontal and vertical directions.

4) After a valve with large-mass was installed in the pipeline, the rigidity distribution in the parallel part of the valve and the pipe determined the changes of fundamental frequency in the system, while the rigidity distribution in the vertical part of the valve and the pipe determined the high order natural frequencies of the system.

5) When the structural responses were predicted by using the response spectrum method with a fixed damping ratio, this resulted in an underestimation of the response of the low damping parts, and a large margin for the predicted results of the high damping parts.

References

Ashok K and Shashi KT (2015), "Comparison of Eigensensitivity and ANN Based Methods in Model Updating of an Eight-Story Building," *Earthquake Engineering and Engineering Vibration*, **14**(33): 453–464.

Cho SG, Furuya O and Kurabayashi H (2019), "Enhancement of Seismic Resilience of Piping Systems in Nuclear Power Plants Using Steel Coil Damper," *Nuclear Engineering and Design*, **350**: 147–157.

Duan Z, Spencer BF, Yan GR, *et al*. (2004), "An Improved Optimal Elemental Method for Updating Finite Element Models," *Earthquake Engineering and Engineering Vibration*, **3**(1): 67–74.

Deng QT and Yang ZC (2019), "Wave Propagation in Submerged Pipe Conveying Fluid," *Acta Mechanica Solida Sinica*, 1–16.

Farajpour A, Farokhi H and Ghayesh MH (2019), "Mechanics of Fluid-Conveying Microtubes: Coupled Buckling and Post-Buckling," *Vibration*, **2**(1): 102–115.

Gupta A, Cho SG, Hong KJ, *et al*. (2019), "Current State of In-Cabinet Response Spectra for Seismic Qualification of Equipment in Nuclear Power Plants," *Nuclear Engineering and Design*, **343**: 269–275.

Jeong YS, Baek ER, Jeon BG, *et al*. (2019), "Seismic Performance of Emergency Diesel Generator for High Frequency Motions," *Nuclear Engineering and Technology*, **50**: 1470–1476.

Kheiri M (2020), "Nonlinear Dynamics of Imperfectly-Supported Pipes Conveying Fluid," *Journal of Fluids and Structure*: 1–18.

Kojima N, Tsutumi Y, Yonekura K, *et al*. (2017), "Seismic Test Result of Motor-Operated Valve Actuators for Nuclear Power Plant," *Proceedings of the ASME 2017 Pressure Vessels and Piping Conference*, July 16-20, 2017, Waikoloa, Hawaii, USA, Paper No. PVP2017-65600.

Kojima N, Tsutumi Y, Yonekura K, *et al*. (2018), "Seismic Test Result of Motor-Operated Butterfly Valve Actuators for Nuclear Power Plant," *Pressure Vessels and Piping Conference*, July 15-20, 2018, Prague, Czech Republic, Paper No. PVP 2018-84219.

Li Q, Li PZ, Du JY, *et al*. (2016), "Exploration of Seismic Qualification Test Method for Nuclear Safety Class Valves," *Nuclear Power Engineering*, **S2**: 61–64. (in Chinese)

Lin RM and Ewins DJ (1994), "Analytical Model Improvement Using Frequency Response Functions," *Mechanical Systems and Signal Processing*, **8**(4): 437–458.

Manolisa GD, Stefanoua G and Markoub AA (2020), "Dynamic Response of Buried Pipelines in Randomly Structured Soil," *Soil Dynamics and Earthquake Engineering*, **128:** 1–11.

Mottershead J and Friswell M (1993), "Model Updating In Structural Dynamics: A Survey," *Journal of Sound and Vibration*, **167**(2): 347–375.

Mueller CS, Boyd OS, Petersen MD, *et al*. (2015), "Seismic Hazard in the Eastern United States," *Earthquake Spectra*, **31**: 85–107.

Nakamura I (2013), "Seismic Safety Capacity of a Piping System With Pipe Supports Based on the Shake Table Test," *Proceedings of the ASME 2013 Pressure Vessels and Piping Conference*, July 14-18, 2013, Paris, France, Paper No. PVP2013-97852.

Naohiro N (2017), "Time History Response Analysis Using Extended Rayleigh Damping Model," *Procedia Engineering*, **199**: 1472–1477.

Nguyena DD, Thusaa B, Hanc TS, *et al*. (2019), "Identifying Significant Earthquake Intensity Measures for Evaluating Seismic Damage and Fragility of Nuclear Power Plant Structures," *Nuclear Engineering and Technology*: 1–14.

Niu J, Zong ZH and Chu FP (2015), "Damage Identification Method of Girder Bridges Based on Finite Element Model Updating and Modal Strain Energy," *Science China Technological Sciences*, **58**(4): 701–711.

Paidoussis MP and Issid NT (1974), "Dynamic Stability of Pipes Conveying Fluid," *Journal of Sound and Vibration*, **33**(3): 267–294.

Sinha JK and Friswell MI (2003), "The Use of Model Updating for Reliable Finite Element Modelling and Fault Diagnosis of Structural Components Used in Nuclear Plants," *Nuclear Engineering and Design*, **223**(1): 11–23.

Sinha JK, Rao AR and Sinha RK (2006), "Realistic Seismic Qualification Using the Updated Finite Element Model for In-Core Components of Reactors," *Nuclear Engineering and Design*, **236**(3): 232–237.

Surh HB, Ryu TY, Park JS, *et al*. (2015), "Seismic Response Analysis of a Piping System Subjected to Multiple Support Excitations in a Base Isolated NPP Building," *Nuclear Engineering and Design*, **292**: 283–295.

Tang Y, Yang TZ and Fang B (2018), "Fractional Dynamics of Fluid-Conveying Pipes Made of Polymer-Like Materials," *Acta Mechanica Solida Sinica*, **31**(2): 119–134.

Wang T, Zhou HM, Zhang XP, *et al*. (2018), "Stability of an Explicit Time-Integration Algorithm for Hybrid Tests, Considering Stiffness Hardening Behavior," *Earthquake Engineering and Engineering Vibration*, **17**(3): 595–606.

Xu WX, Sun JJ, Yang WS, *et al*. (2014), "Shaking Table Comparative Test and Associated Study of a Stepped Wall-Frame Structure," *Earthquake Engineering and Engineering Vibration*, **13**(3): 471–485.

Xue SD, Shan MY, Li XY, *et al*. (2019), "Shaking Table Test and Numerical Simulation of an Isolated Cylindrical Latticed Shell Under Multiple-Support Excitation," *Earthquake Engineering and Engineering Vibration*, **18**(3): 611–630.

Zhang SW, Shen SS, Liu LL, *et al*. (2015), "Test and Research for Integrity Evaluation of Nuclear Pipe System Under Seismic Effect," *Nuclear Power Engineering*, **36**(5): 41–44. (in Chinese)